Search Hits Help

A New Type of Frequency Chain and Its Application to Fundamental Frequency Metrology

Thomas Udem[1], Jörg Reichert[1], Ronald Holzwarth[1], Scott Diddams[2], David Jones[2], Jun Ye[2], Steven Cundiff[2], Theodor Hänsch[1], and John Hall[2]

[1] Max-Planck Institut für Quantenoptik, Garching/Germany
[2] JILA, University of Colorado and National Institute of Standards and Technology, Boulder, CO/USA

Abstract. A suitable femtosecond (fs) laser system can provide a broad band comb of stable optical frequencies and thus can serve as an rf/optical coherent link. In this way we have performed a direct comparison of the $1S-2S$ transition in atomic hydrogen at 121 nm with a cesium fountain clock, built at the LPTF/Paris, to reach an accuracy of 1.9×10^{-14}. The same comb-line counting technique was exploited to determine and recalibrate several important optical frequency standards. In particular, the improved measurement of the Cesium D_1 line is necessary for a more precise determination of the fine structure constant. In addition, several of the best-known optical frequency standards have been recalibrated via the fs method. By creating an octave-spanning frequency comb a single-laser frequency chain has been realized and tested.

1 Introduction

A frequency comb of equally spaced continuous wave laser frequencies can be used to measure large differences between laser frequencies simply by multiplying the known spacing of the comb with the number of modes in between. The use of mode-locked lasers as optical comb generators was already reported over 20 years ago [1]. As the spectral width of such a comb scales inversely with the (Fourier limited) pulse duration, its application was limited to comparatively small frequency differences like the 1028 MHz fine structure splitting of the sodium 4d level [1]. This limited bandwidth situation changed fundamentally with the discovery of self-mode locking in Ti:Sapphire lasers [2], as explained by Kerr-lens mode-locking [3], and the development of designs to produce $\approx$ 10 femtosecond pulses [4]. Recently pulses shorter then 6 fs have been created directly from a Ti:Sapphire laser oscillator [5,6] with the help of special dispersion-compensating mirrors. By using self-phase modulation in specially designed optical fibers [7,8,9,10,11] frequency combs have been created with bandwidth in excess of one optical octave. Even after spectral broadening the comb lines remain surprisingly equidistant to an extreme degree [13]. Those combs can be used to measure the frequency gap between a laser frequency f and its second harmonic $2f$ [14,15,16,17,18,19]. This principle allows the realization of a compact single-laser frequency chain which can be used to measure almost any optical frequency with the same compact apparatus. In the time domain, the

output of a mode-locked femtosecond laser may be considered as a continuous carrier wave that is strongly amplitude modulated by a periodic pulse envelope function. If such a pulse train and the light from a cw laser are combined on a photo detector, the beat note between the carrier wave and the cw oscillator is, in fact, observed in a stroboscopic sampling scheme. The detector signal will thus reveal a slow modulation at the beat frequency modulo the sampling rate or pulse repetition frequency. A similar idea based on the stroboscopic sampling scheme has been reported previously by Chebotayev et al. [20].

2 Kerr-Lens Mode-Locked Lasers

The spectrum emitted by a mode locked laser consists of a comb of laser frequencies that may be identified with the active modes of the laser cavity [21]. The mode separation in a dynamically stable cavity of length L is calculated from the boundary condition that is imposed on the round trip phase delay:

$$2Lk(\omega_n) = 2\pi n \tag{1}$$

This equation fixes the optical frequency $\omega_n = 2\pi n v_p(\omega_n)/2L$ and the wave number $k(\omega_n) = \omega_n/v_p(\omega_n)$ of the nth cavity mode, where $v_p(\omega_n)$ is the phase velocity for a monochromatic wave at ω_n. The following expansion about some mean frequency ω_m is generally used to take dispersion into account:

$$2L\left[k(\omega_m) + k'(\omega_m)(\omega_n - \omega_m) + \frac{k''(\omega_m)}{2}(\omega_n - \omega_m)^2 + ...\right] = 2\pi n \tag{2}$$

The mode separation $\omega_r \equiv \omega_{n+1} - \omega_n$ is obtained by subtracting this expression from itself after n is replaced by $n+1$:

$$k'(\omega_m)\omega_r + \frac{k''(\omega_m)}{2}\left((\omega_{n+1} - \omega_m)^2 - (\omega_n - \omega_m)^2\right) + ... = 2\pi/2L \tag{3}$$

A constant mode spacing that is independent of n is mandatory for precise optical frequency measurements. This is obtained, if all terms in the expansion of the wave vector $k(\omega)$ vanish except for the constant term $k(\omega_m)$ and the group velocity term $v_g^{-1} = k'(\omega_m)$ [21]. These higher-order terms are exactly the ones that reshape the pulse envelope. The detection of a temporal pulse envelope, that stays constant for hours in within the laser cavity, is therefore a clear prerequisite for the absence of dispersion terms that would perturb the regular grid of laser frequencies. The mode separation then turns into the known expression for the free spectral range of a multi mode laser $\omega_r = 2\pi v_g/2L$. This expression is actually the inverse pulse round trip time $T^{-1} = v_g/2L = \omega_r/2\pi$, i.e. the rate at which copies of the same pulse appear at the output coupler. The mode spacing is therefore readily experimentally accessible as the pulse repetition frequency. The arbitrariness about the choice of ω_m is removed by using an experimental value for the repetition rate rather than a chosen value for ω_m to calculate v_g.

Search Hits Help

In Kerr-lens mode-locked lasers [3] a combination of prism pairs or specially designed mirrors [22], are used to compensate for the positive group velocity dispersion $k''(\omega_m)$ (GVD) of the laser crystal and mirrors etc. The remaining perturbations of the regular grid of modes, due to a imperfect compensation of the GVD and the presence of higher order terms, are zeroed by mode pulling[1]. With Kerr-lens mode-locking this pulling is achieved by exploiting a Kerr-lens that persists only in the presence of an intense short pulse. The cavity is designed to make the cavity less lossy if the Kerr-lens is present. The result is a short pulse with a stable envelope that bounces back and forth between the cavity end mirrors. In that regime the modes do not only maintain a constant frequency separation between them but even a constant relative phase (up to a phase advance of $\omega_r t$).

The achievable pulse length is determined by the total number of modes that can contribute to the pulse. The broader the frequency comb the shorter the possible pulse length, ideally reaching the so-called Fourier limit. In fact, the spectral width is usually limited by the width over which the GVD and higher order terms can be compensated for by mode pulling [5,6]. Cavity modes that are outside this bandwidth are suppressed without the help of the Kerr-lens effect and do not oscillate.

3 Femtosecond Frequency Combs

A strict derivation of the comb properties is not feasible as it depends on the special dispersion characteristics of the laser cavity and these data are not accessible with the desired degree of accuracy. Instead we only assume that the laser emits a stable coherent pulse train without any detailed consideration of how this is possible. Further we assume that the electric field $E(t)$, measured for example at the output coupler, can be written as the product of a periodic envelope function $A(t)$ and a carrier wave $C(t)$:

$$E(t) = A(t)C(t) + c.c. \tag{4}$$

The envelope function defines the pulse repetition time $T = 2\pi/\omega_r$ by demanding $A(t) = A(t-T)$. Inside the laser cavity the difference between the group velocity and the phase velocity shifts the carrier with respect to the envelope after each round trip. The electric field is therefore in general not periodic with T. To obtain the spectrum of $E(t)$ the Fourier integral has to be calculated:

$$\tilde{E}(\omega) = \frac{1}{\sqrt{2\pi}} \int_{-\infty}^{+\infty} E(t) e^{i\omega t} dt \tag{5}$$

Separate Fourier transforms of $A(t)$ and $C(t)$ are given by:

$$\tilde{A}(\omega) = \sqrt{2\pi} \sum_{n=-\infty}^{+\infty} \delta\left(\omega - n\omega_r\right) \tilde{A}_n$$

[1] More precisely the slight negative GVD in the cold cavity compensates with the Kerr nonlinearity to sustain an optical soliton.

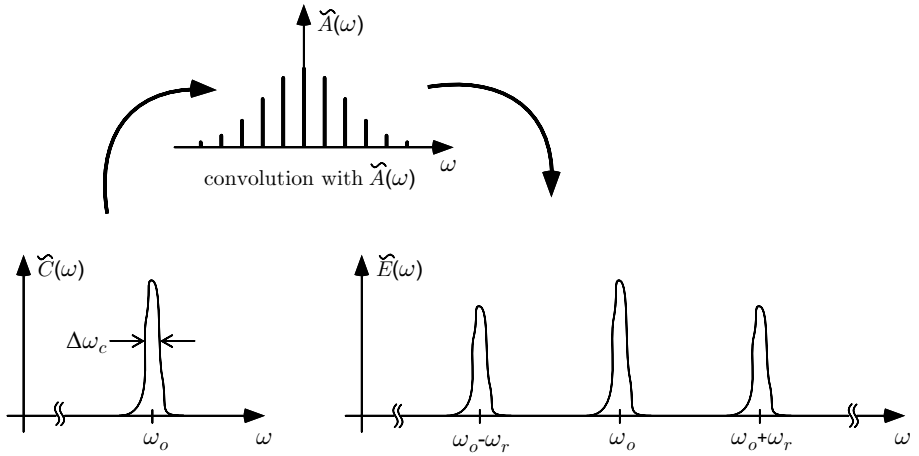

Fig. 1. The spectral shape of the carrier function (left) assumed to be narrower than the pulse repetition frequency $\Delta\omega_c \ll \omega_r$ and the resulting spectrum according to Eqn. 7 after modulation by the envelope function (right)

$$\tilde{C}(\omega) = \frac{1}{\sqrt{2\pi}} \int_{-\infty}^{+\infty} C(t) e^{i\omega t} dt \tag{6}$$

A periodic frequency chirp imposed on the pulses is accounted for by allowing a complex envelope function $A(t)$. Thus the "carrier" $C(t)$ is defined to be whatever part of the electric field that is non-periodic with T. The convolution theorem allows us to calculate the Fourier transform of $E(t)$ from $\tilde{A}(\omega)$ and $\tilde{C}(\omega)$:

$$\begin{aligned} \tilde{E}(\omega) &= \frac{1}{\sqrt{2\pi}} \int_{-\infty}^{+\infty} \tilde{A}(\omega') \tilde{C}(\omega - \omega') d\omega' + c.c. \\ &= \sum_{n=-\infty}^{+\infty} \tilde{A}_n \tilde{C}\left(\omega - n\omega_r\right) + c.c. \end{aligned} \tag{7}$$

Up to the scaling factors $\tilde{A}_n$ this sum represents a periodic spectrum in frequency space. If the spectral width of the carrier wave $\Delta\omega_c$ is much smaller than the mode separation ω_r, Eqn. 7 represents a regularly spaced comb of laser modes with identical spectral line shapes, namely the line shape of $\tilde{C}(\omega)$ (see Fig. 1). If $\tilde{C}(\omega)$ is centered at say ω_c then the comb is shifted from containing only exact harmonics of ω_r by ω_c. The center frequencies of the mode members are calculated from the mode number n [23,24,21]:

$$\omega_n = n\omega_r + \omega_c \tag{8}$$

Search Hits Help

The measurement of the frequency offset ω_c [16,17,18,19] as described below usually yields a value modulo ω_r so that renumbering the modes will restrict the offset frequency to $0 \leq \omega_o \leq \omega_r$:

$$\omega_n = n\omega_r + \omega_o \qquad n = \text{a large integer} \tag{9}$$

This equation maps two radio frequencies ω_r and ω_o onto the optical frequencies ω_n. While ω_r is readily measurable, ω_o is not easy to access unless the frequency comb contains more than an optical octave, as shown in section 7. The individual modes can be separated, for example with an optical grating, if the spectral width of the carrier function is narrower than the mode separation: $\Delta\omega_c \ll \omega_r$. This condition is easy to satisfy, even with a free running Ti:Saphire laser.

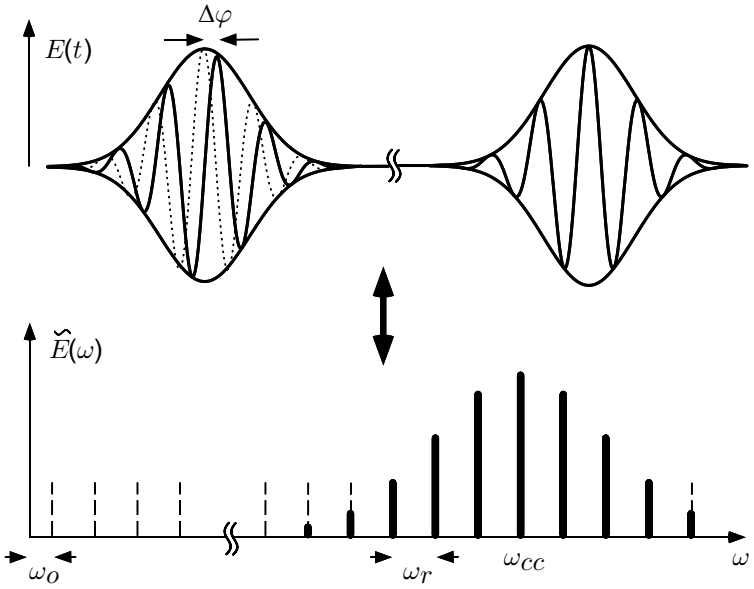

Fig. 2. Consecutive pulses of a chirp free pulse train ($A(t)$ real) and the corresponding spectrum. Because the carrier propagates with a different velocity within the laser cavity than the envelope (phase- and group velocity), the electric field does not repeat itself after one round trip. A pulse-to-pulse phase shift $\Delta\varphi$ results in an offset frequency of $\omega_o = \Delta\varphi/T$

Now let us consider two instructive examples of possible carrier functions. If $C(t) = e^{-i\omega_{cc}t}$ the output the line shapes of the individual modes are delta functions $\tilde{C}(\omega) = \delta(\omega - \omega_{cc})$. The frequency offset ω_c of Eqn. 8 is identified with ω_{cc}. According to Eqn. 4 after each round trip the carrier will shift with respect to the envelope by $\Delta\varphi = \arg(C(t-T)) - \arg(C(t)) = \omega_{cc}T$ so that the frequency offset is given by $\omega_{cc} = \Delta\varphi/T$ [23,24,21]. In a typical laser cavity this

Search Hits Help

pulse-to-pulse carrier-envelope phase shift is much larger than 2π but measurements [25,17] usually yield a value modulo 2π. The restriction $0 \leq \Delta\varphi \leq 2\pi$ is synonymous with the restriction $0 \leq \omega_o \leq \omega_r$ introduced earlier. Figure 2 sketches this situation in the time domain for a chirp free pulse train.

As the second example consider a train of half-cycle pulses, for example:

$$E(t) = E_o \sum_k e^{-\left(\frac{t-kT}{\tau}\right)^2} \tag{10}$$

In this case the electric field would be repetitive with the round trip time. Therefore $C(t)$ is a constant and its Fourier transform is a delta function centered as $\omega_c = 0$. If it becomes possible to build a laser able to produce a stable pulse train of that kind, all the comb frequencies would become exact harmonics of the pulse repetition rate. Obviously, this would be an ideal situation for optical frequency metrology.

These examples are instructive, but it is important to note that experimentally we neither rely on a strictly periodic electric field nor on the assumption of a chirp free pulse train. The strict periodicity of the spectrum as stated in Eqn. 7 and the possibility to resolve single modes are the only requirements that enable the fs laser system to achieve precise optical to radio frequency conversions.

In a real laser a pulse train with a chirp mostly synchronized with the repetition rate will be emitted. That is because the same pulse is maintained in the laser cavity practically for an infinite time without degradation. A pulse chirp that is monotonically increasing or decreasing from pulse to pulse would monotonically shift the emitted spectrum in one direction and is therefore ruled out. All that is left is a possible pulse to pulse phase shift (giving rise to a frequency offset of the comb) and noise on the chirp, the pulse shape and the intensity. The noise processes will either broaden the individual modes or impose amplitude noise on their relative intensities. Provided that the noise on the chirp is small as compared to the mode spacing none of these processes will change the regular spacing of the comb. This is in fact the only feature that we rely on for optical frequency metrology because ω_r and ω_o of Eqn. 9 are servo controlled in those experiments. In fact recent experiments performed in our Garching laboratory [26] confirm the model used here and set an upper limit on the mode spacing constancy of 3 parts in 10^{17} even for a free running femtosecond laser. In the same work the equality of the mode separation and the pulse repetition frequency was established with an upper limit of 6 parts in 10^{16}.

4 Spectral Broadening by Self-Phase Modulation

The spectral width of a pulse train emitted by a femtosecond laser can be significantly broadened in a single mode fiber [27]. This process that maintains the mode structure is described in the time domain by the optical Kerr effect or self-phase modulation. The first discussion is simplified by assuming an unchanging pulse-shape under propagation. After propagating the length l the intensity dependent refractive index $n(t) = n_o + n_2 I(t)$ leads to a self induced phase shift

Search Hits Help

of

$$\Phi_{NL}(t) = -n_2 I(t)\omega_c l/c \qquad \text{with } I(t) = |A(t)|^2. \tag{11}$$

This time dependent phase shift leads to a frequency modulation that is proportional to the time derivative of the self induced phase shift $\dot{\Phi}_{NL}(t)$. For fused silica with its positive Kerr coefficient $n_2 = 2.5 \times 10^{-16}$ cm^2/W [28] the leading edges of the pulses are creating extra frequencies shifted to the red ($\dot{\Phi}_{NL}(t) < 0$) while the trailing edges causes blue shifted frequencies to emerge. Self-phase modulation modifies the envelope function according to

$$A(t) \longrightarrow A(t)e^{i\Phi_{NL}(t)}. \tag{12}$$

Because $\Phi_{NL}(t)$ has the same periodicity as $A(t)$ the comb structure of the spectrum, as derived in section 3, is not affected. In an optical fiber self-phase modulation can be quite efficient even though the nonlinear coefficient in fused silica is comparatively small. This is because the fiber core carries a high intensity over an extended length.

This simplified picture of self-phase modulation neglects dispersion, time-delayed nonlinearities and shock formation which is all known to occur in optical fibers. While n_2 in fused silica is at least as fast as a few fs, the GVD broadens the pulses as they travel along the fiber so that the available peak power P_o is decreased. Effective self-phase modulation however takes place when the so called dispersion length is much smaller then the nonlinear length whose ratio is given by [27]

$$R = \frac{L_D}{L_{NL}} = \frac{n_2\omega_c P_o T_o^2}{cA_{eff}|k''(\omega_c)|} \tag{13}$$

where T_o and A_{eff} are the initial pulse duration and the effective fiber core area [27] calculated from the radial intensity distribution[2]. In the dispersion dominant regime $R \ll 1$ the pulses will disperse before any significant nonlinear interaction can take place while for $R \gg 1$ dispersion can be neglected as an inhibitor of self-phase modulation. Of course here we are considering the case of a physical fiber longer than either $L_D = T_o^2/|k''(\omega_c)|$ or $L_{NL} = cA_{eff}/n_2\omega_c P_o$.

So we see that spectral broadening of the comb [29,30] is achieved by imposing a large frequency chirp on each of the pulses. Provided that the coupling efficiency into the fiber is stable, the periodicity of the pulse train is maintained. The discussion of section 3 is thus equally valid if the electric field $E(t)$ as measured for example at the fiber output facet instead of the laser output coupler. As described below we have used a frequency comb widened to more than 45 THz by a conventional single mode fiber to perform the first phase coherent vacuum UV to radio frequency comparison in our Garching laboratory [16,31]. In recent experiments we have confirmed that the fiber does not affect the mode spacing constancy within our experimental uncertainty of a few parts in 10^{18} [13].

[2] $A_{eff} = \pi w_o^2$ for a Gaussian beam with radius w_o.

5 Photonic Crystal Fibers

Very efficient spectral broadening can be observed in photonic crystal fibers (PCF) [7,8,9,10,11]. A PCF uses a triangular array of submicron-sized air holes running the length of a silica fiber to confine light to a pure silica region embedded within the array [7]. The large refractive index contrast between the pure silica core and the "holey" cladding, and the resultant strong nature of the optical confinement, allows the design of fibers with characteristics quite different from those of conventional fibers. The larger index contrast enables use of a small core size, and the increased energy concentration leads to increased nonlinear interaction of the guided light with the silica. As a considerable fraction of the mode travels as an evanescent wave inside the air holes, the waveguide dispersion can be designed to be strong enough to substantially compensate the material dispersion. As a result, fs pulses travel further in these fibers before being dispersed which further increases the nonlinear interaction. Consequently, substantially broader spectra can be generated in PCFs at relatively low peak powers [9,10,11]. Other processes like stimulated Raman and Brillouin scattering or shock wave formation that might spoil the usefulness of these broadened frequency combs are probably present. Indeed, in an experiment using 8 cm of PCF and 73 fs pulses at 75 MHz repetition rate from a Mira 900 system (Coherent Inc.) we have seen an exceptionally broad spectrum from 450 to 1400 nm with excessive broadband noise, way above the shot noise. Using 25 fs pulses at a repetition rate of 625 MHz for the frequency chain reported below, this extra broadband noise was suppressed so as to enable us to phase lock the comb. As an additional data point, the JILA laser (Kapteyn-Murnane Labs model TS) with 100 MHz repetition rate leads to a comfortable operating range near 25 mW transmitted power, where the 1064 nm and 532 nm beats with a CW laser were both adequate. Further power increases rapidly decreased the S/N ratio. Comparing the several Boulder sources, one finds the best operation near 250 pJ per pulse, basically independent of repetition rate for $\approx$ 50 fs pulses. The detailed nature of interesting broadband excess noise is not yet known. Thus there is still a little "art" in the proper use of the fiber broadening process for metrology.

6 Phase-Locking the Frequency Comb

For most applications of the frequency comb it is desirable to fix one of the modes in frequency space and to phase-lock the pulse repetition rate simultaneously. For this purpose it is necessary to control the phase velocity (more precisely the round trip phase delay) of that particular mode and the group velocity (more precisely the round trip group delay) independently. A piezo driven folding mirror changes the cavity length L and shifts all modes proportional to their absolute frequency $\Delta\omega_n = \omega_n \Delta L/L$, as the additional path in air has a negligible dispersion. A mode-locked laser that uses two intra-cavity prisms to produce the negative group velocity dispersion necessary for Kerr-lens mode-locking provides us with a means for independently controlling the pulse

Search Hits Help

repetition rate. To change the mode separation without changing the absolute frequency of say ω_n, we use a second piezo-transducer to tilt the mirror slightly at the dispersive end of the cavity where the modes are horizontally dispersed. The vertical pivot ideally corresponds to the mode ω_n [21]. We thus introduce an additional phase shift $\Delta\psi$ proportional to the frequency distance from ω_n, which displaces the pulse in time and thus changes the round trip group delay. In the frequency domain one could argue that the length of the cavity stays constant for the mode ω_n while higher (lower) frequency modes experience a longer (shorter) cavity (or vice versa, depending on the sign of $\Delta\psi$). With our Coherent Mira 900 system the position of the pivot did not seem to be important and could even be placed next to the mirror. Also the slight misalignment of the laser cavity introduced only a negligible loss of power. In the alternative case where only dispersion compensation mirrors are used to produce the negative group velocity dispersion, one can modulate the pump power or manipulate the Kerr lens by slightly tilting the pump beam [19] in order to alter ω_o. The cavity length then is used to control the repetition rate. Although the two controls (i.e. cavity length and pump power) are not orthogonal they affect the round trip group delay T and the round trip phase delay differently. Further, the pump control loop can be rather fast compared with the PZT-driven length correction. Thus we can control both, ω_o and ω_r.

In a different approach, the JILA group has locked the fs laser's two degrees of freedom using information from beats with our stable Nd:YAG/I_2 reference laser system, without using an rf source. In this work, the beat at 1064 nm mainly controlled the position of one optical comb line, while the 532 nm beat was used to control the repetition rate. This frequency information was used to tightly lock, eventually phase-lock, the laser cavity length via the 1064 nm beat. As this PZT motion also affects the repetition rate somewhat, we found it attractive to use a frequency-based lock for the 532 nm-derived information, applying it to the "twister" PZT to mainly affect the repetition rate. Unfortunately the comb line chosen for absolute frequency stabilization, at 1064 nm, is not really near the center of the fiber-broadened spectrum, which led to a serious level of non-orthogonality. This was handled by preparing an appropriate linear combination of the two signals for the two transducers and their servo systems. We obtained rms frequency noise (1s) below 1 Hz for the 1064 nm beat and about 180 Hz for the green beat [33]. Basically this two-laser system offers about 4 million stable optical frequencies, with 100 MHz optical frequency separations, each with linewidths $\approx$ 100 Hz and below, and with a stability improving in time, ideally following the Nd:YAG/I_2 reference which shows an Allan Deviation of $\approx 4 \times 10^{-15}$ at 700 s. By measuring the repetition rate against the NIST frequency standard, all of these comb lines are known in absolute frequency. Alternatively and interestingly, the repetition rate should form a stable optical clock with its output at 100 MHz. Such a result, translating frequency stability gained in the optical domain into the microwaves and rf, is made possible by the broad, octave-spanning fs comb. Using our new fiber optic connection to the NIST Frequency Standard, it will be fascinating to compare our optically-

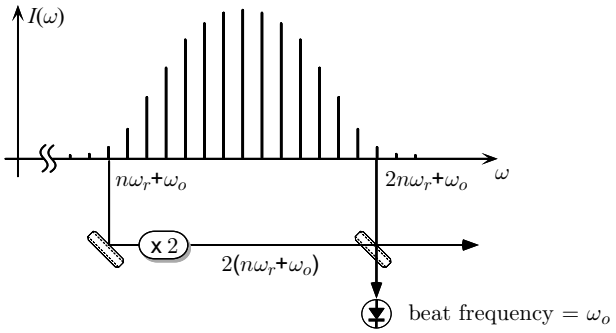

Fig. 3. The offset frequency ω_r that displaces the modes of an octave spanning frequency comb from being exact harmonics of the repetition rate ω_r is measured by frequency doubling some modes at the "red" side of the comb and beat them with modes at the "blue" side

derived clock output stability with that of the NIST rf standard system. Already the rf stability is not worse than the best other source available to us.

7 Self-calibrated Optical Combs: Absolute Optical Frequencies

Being able to control ω_o and ω_r is not sufficient if we don't know their values. The repetition rate ω_r is simply measured by a photo detector at the output of either the laser or the fiber. To measure the offset frequency ω_o, a mode $n\omega_r + \omega_o$ on the "red" side of the comb is frequency doubled to $2(n\omega_r + \omega_o)$. If the comb contains more than an optical octave there will be a mode with the mode number $2n$ oscillating at $2n\omega_r+\omega_o$. As sketched in Fig. 3 we take advantage of the fact that the offset frequency is common to all modes[3] by creating the beat frequency (=difference frequency) between the frequency doubled "red" mode and the "blue" mode to obtain ω_o. This method allowed the construction of a very simple frequency chain [14,15,16,17,18,19] that eventually operated with a single laser. It occupies only 1 square meter on our optical table with considerable potential for further miniaturization. At the same time it supplies us with a reference frequency grid across much of the visible and infrared spectrum.

The system sketched in Fig. 3 is implemented in Garching with a Ti:sapphire 25 fs ring laser (GigaOptics, model GigaJet) with modes that are separated by $\omega_r = 2\pi$ 625 MHz. This makes it easy to distinguish them with a commercial wavemeter. While the ring design makes it almost immune to feedback from the fiber, the high repetition rate increases the available power per mode. The highly efficient spectral broadening of the PCF compensates for the decrease of available pulse peak power connected with a high repetition rate. To generate an octave spanning comb we have coupled 190 mW average power through 35 cm PCF.

[3] This is another way of saying that the modes are equally spaced.

Search Hits Help

The pump beam intensity (Verdi, Coherent Inc.) is controlled by an EOM (LM 0202, Gsänger). With 7 W of pump power we achieve above 650 mW average power from the femtosecond laser.

The infrared part of the spectrum at the fiber exit is separated from the green part with the help of a dichroic mirror, and passed through a $3 \times 3 \times 7$ mm^3 AR coated KTP crystal properly cut for frequency doubling with ≈ 1060 nm input. The harmonic green is recombined on a polarizing beam splitter with the green part from the direct fiber output. For the green comb part an optical delay line is included to match the optical path lengths. In the JILA setup [18], an AOM was also introduced in this arm to displace the interesting beat frequency region away from zero (see Fig.5). The polarization axes of the recombined light are mixed using a rotatable polarizer. A grating which serves as 5 nm wide bandpass filter selects the wavelengths around 530 nm. A beat signal with a signal to noise ratio exceeding 40 dB in 400 kHz bandwidth has been obtained at Garching. The offset frequency is phase locked with the help of an EOM in the pump beam while the repetition rate ω_r is phase locked with a PZT mounted folding mirror. By this means the absolute frequency of each of the modes is phase coherently linked to the rf reference and known with the same relative precision.

To use this calibrated frequency grid, a low noise beat signal between one of the modes with a cw laser has to be created. This is done by spectrally filtering the comb to prevent most of the unused modes, that only produce shot noise, from impinging on the photo detector. The rotatable polarizer, that works as an adjustable beam splitter, is then used to maximize the signal to noise ratio. In some cases a Phase-Tracking Oscillator can help to guarantee accurate counting. Some of the details are found in Ref. [21].

The single-laser $f : 2f$ frequency chain now appears as the natural endpoint of a thirty-year development to measure absolute optical frequencies, using intervals between harmonics or subharmonics of laser frequencies (see later). But for the first demonstration of the self-referenced frequency comb concept performed in Garching, not too long ago [16], when photonic crystal fibers were not yet widely available, we managed to obtain spectral broadening by use a regular single mode fiber. At that time we could bridge a frequency interval of 50 THz at the most when seeding the fiber with a commercial mode-locked laser (Coherent model Mira 900) that had a repetition rate of 75 MHz and a measured pulse duration of 73 fs. Interestingly, the shorter pulses from the JILA laser led to broadening beyond 100 THz, also using a standard fiber [30]. As shown in Fig. 4 the 50 THz comb is used to fix the frequency difference $0.5f$ between two laser diodes at $4f$ (848 nm) and $3.5f$ (969 nm). One laser diode is phase locked to the fourth harmonic of an infrared HeNe laser at f (3.39 μm) and the other is frequency doubled to obtain $7f$. At that stage all lasers but the the HeNe laser are phase locked to another laser in the chain. We close the chain by phase locking the remaining laser by controlling its frequency f such that the sum of f and $7f$ equals $8f$ as produced by frequency doubling the laser diode at $4f$. Only after closing the last phase locked loop are the relations between absolute frequencies

Search Hits Help

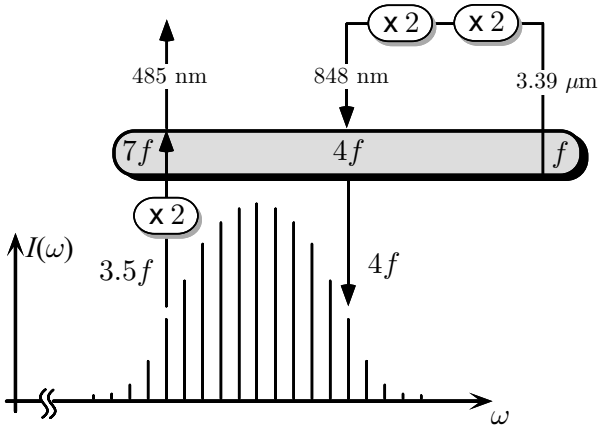

Fig. 4. The first self-referenced frequency chain that has been used in Refs. [16,19,31] uses an optical frequency interval divider (oval symbol) [34] that fixes the relation between the frequencies f, $4f$ and $7f$ by locking $f+7f$ to $2\times 4f$. The 3.39 μm laser at f is locked through the divider after the frequency comb locked the difference between $3.5f$ and $4f$

as mentioned precisely fulfilled. We can then set the frequency of the HeNe laser, and all other lasers in the chain, by setting the frequency difference between the laser diodes $4f-3.5f=0.5f$ with a cesium atomic clock that controls the mode spacing. We have used this frequency chain for an improved measurement of the hydrogen 1S-2S transition frequency at 2466 THz [16,31]. We excite this transition with two photons from a frequency doubled dye laser at 486 nm. To enable us to use the $7f$ output of the frequency chain shown in 4 we introduced a second smaller frequency gap that is measured with the same frequency comb. As described elsewhere in this volume [35] we use a sophisticated line shape model [36,35] to obtain [31]

$$f_{1S2S} = 2\ 466\ 061\ 413\ 187\ 103(46)\ \text{Hz} \tag{14}$$

for the hyperfine centroid. To achieve this accuracy we made use of a transportable cesium fountain clock [32] constructed by the group of A. Clairon at the *Laboratoire Primaire du Temps et des Fréquences* (LPTF). This measurement represents now the most precise measurement of an optical frequency and provides the first phase coherent link from the vacuum UV (121 nm) to the radio frequency domain. A previous measurement [37] of this transition also serves as an independent test of the previous harmonic frequency chains at Garching and at the Physikalisch Technische Bundesanstalt Braunschweig/Germany to within 3.4 parts in 10^{13}.

After the first successful testing of the comb properties at Garching [26] other groups worldwide also saw the single-laser $f:2f$ self-calibrated frequency chain as a highly attractive desirable approach to measuring absolute optical frequencies. It has long been known that a white light continuum is produced when an

Search Hits Help

(amplified) femtosecond laser pulse is focused into a nonlinear dielectric medium with an intensity-dependent refractive index. Experiments carried out in early 1997 [38] demonstrated conclusively that such white light continuum pulses can be mutually phase-coherent, and a universal optical frequency comb synthesizer with a train of such pulses was envisioned by one of us (T.W.H.) at that time. However, pulses intense enough could not be produced with a sufficiently high repetition rate that could have allowed one to separate out a single mode. In May 1999, researchers at Lucent Technology announced the generation of white light continuum pulses directly from a low-power femtosecond laser oscillator with the help of a microstructured silica fiber [11]. It was then obvious to some of us that such fibers would produce an octave-spanning frequency comb, and the Garching and Boulder teams entered a friendly race to obtain a fiber sample. The Boulder team won this race by a few weeks and obtained its fiber sample from Lucent in October 1999 to demonstrate the first octave-spanning self-referenced frequency comb [14,17,18]. The Garching group obtained a photonic crystal fiber a few weeks later from P. Russell at Bath University [12] and successfully implemented a single-laser frequency "chain" in November 1999 [15,16,19].

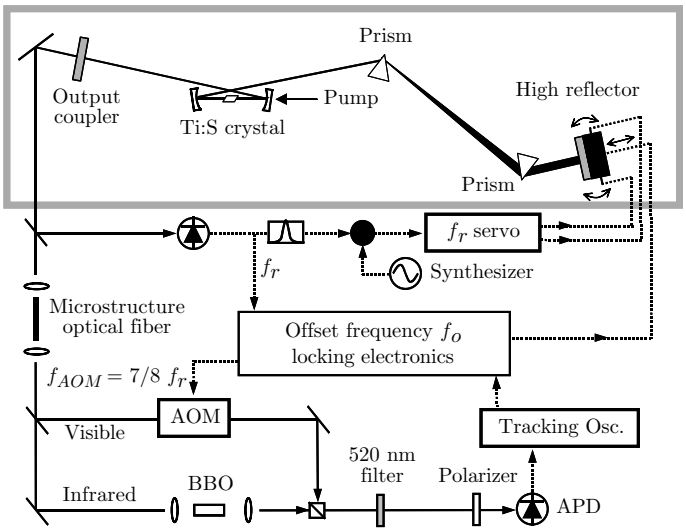

Fig. 5. Experimental setup for locking the offset frequency ω_o. The femtosecond laser is located inside the shaded box. Solid lines represent optical paths, and dashed lines show electrical paths. The high-reflector mirror is mounted on a transducer to provide both tilt and translation

The JILA implementation of this technique is illustrated in Fig. 5 [18]. For the first measurement ω_r was phase locked to a precise radio frequency reference (a GPS controlled Rb standard) but knowledge and control of ω_o was not required. The entire comb was allowed to freely "float" and δ_1 and δ_2 were measured

Search Hits Help

as two heterodyne beats. One beat was between ω_{1064}, a I_2 stabilized Nd:YAG laser and an infrared comb mode and the other beat was between the frequency doubled Nd:YAG laser and a green comb mode. With only the mode spacing of the fs comb fixed, the variations of the δ_1 and δ_2 are correlated as ω_o fluctuates. This correlated noise, and therefore any dependence on ω_o, is removed before counting by preparing either the difference or sum of δ_1 and δ_2. Measurements using this technique yielded a frequency for the $^{127}I_2$ R(56) $32-0$ a_{10} transition of 563 260 223 514(5) kHz. The dominant sources of uncertainty were the realization of the optical frequency (± 4 kHz) in addition to the microwave frequency (± 2.2 kHz) that controls ω_r. Once the very stable iodine-stabilized CW-YAG is measured in this fashion its realization is no longer a limitation, and any other optical frequency that falls within the bandwidth of the comb can be measured with respect to the iodine standard. This enabled the concurrent measurement of the 633 nm HeNe/I_2 [39] and the 778 nm Rb 2-photon [40] standard [17].

As described earlier, a more elegant technique exists to measure and control the offset frequency ω_o, while furthermore eliminating the need for any auxiliary CW lasers. As shown, the comparison of frequency-doubled low frequency comb components from the fiber can be heterodyned with the directly generated comb components near twice the optical frequency to yield ω_o. With the AOM operating at 7/8 of the 90 MHz repetition rate, the JILA team could establish the condition of zero offset of the comb-lines from harmonics of the repetition frequency, i.e. $\omega_o = 0$. Alternatively, thanks to the digital frequency synthesis employed, we could fix the offset frequency to be a rational fraction of the inter-comb-line spacing. This provides a defined cycle period for the carrier-envelope phase-slip closure cycle, which may be useful in experiments designed to elucidate a dependence on the carrier-envelope phase. The Garching team achieved this ability to select an arbitrary value of ω_o (including $\omega_o = 0$) by the use of an auxiliary frequency doubled Nd:YAG laser [19].

8 Accuracy Tests of the fs Laser Comb Approach

Previously we have shown that the repetition rate of a mode locked laser equals the mode spacing to within the experimental uncertainty of a few parts in 10^{16} [26] by comparing it with a second frequency comb generated by an efficient electro-optic modulator [41]. Furthermore the uniform spacing of the modes was verified [26] even after further spectral broadening in a standard single mode fiber on the level of a few parts in 10^{18} [13]. To check the integrity of the femtosecond approach we compared the $f:2f$ interval frequency chain as sketched in Fig. 3 with the more complex version of Fig.4 [19]. We used the 848 nm laser diode of Fig. 4 and a second 848 nm laser diode locked to the frequency comb of the $f:2f$ chain. The frequencies of these two laser diodes measured relative to a quartz oscillator, that was used as a radio frequency reference for the frequency combs, are 353 504 624 750 000 Hz and 353 504 494 400 000 Hz for the $f:2f$ and the $3.5f:4f$ chain respectively. We expect a beat note between the two 848 nm laser diodes of 130.35 MHz which was measured with a radio frequency

Search Hits Help

counter (Hewlett Packard, model 53132A) referenced to the same quartz oscillator. In all the measurements described here we use additional frequency counters to detect cycle slips in the phase locked loops (see for example [19]). We exclude data with cycle slips from evaluation.

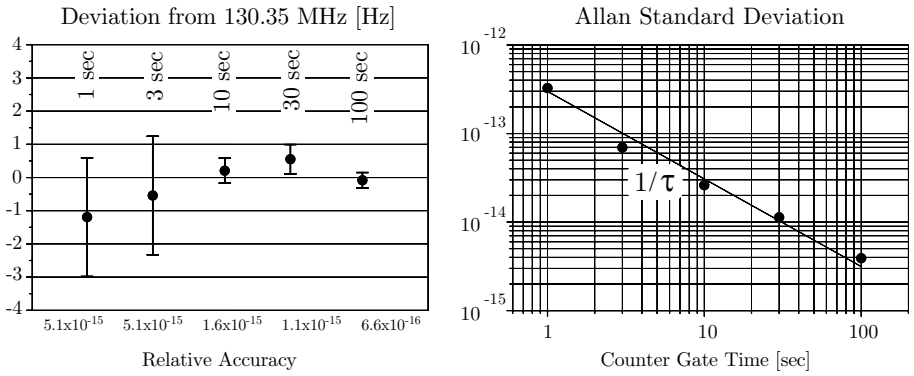

Fig. 6. Left: Deviation of the averaged beat note between the two frequency chains from the expected value for various counter gate times. Right: Measured Allan standard deviation between the two chains as a function of the counter gate time

After averaging all data we obtained a mean deviation from the expected beat frequency of 71 ± 179 mHz at 354 THz. This corresponds to a relative uncertainty of 5.1×10^{-16}. No systematic effect is visible at this accuracy and the distributions of data points look almost ideally Gaussian for sufficiently large data sets. Fig. 6 shows the measured Allan standard deviation [42], which measures the stability of one chain against the other, for counter gate times[4] of 1, 3, 10, 30 and 100 s. As both 354 THz signals are phase locked to each other (via the quartz oscillator) and the rms phase fluctuation is expected to be constant in time, the Allan standard deviation should fall off like the inverse counter gate time. Presumably the larger $3.5f : 4f$ chain is limiting the relative stability as it includes large range ($\pm 1024\ \pi$) phase detectors necessary to compensate for the low servo bandwith available for some of the lasers. In addition the large frequency chain of Fig. 4 is resting on two separate optical tables whose relative position was not controlled. Another source of instability could be the specified 1.5×10^{-13} Allan standard deviation (within 1 s) of the quartz oscillator together with time delays present in both systems.

Another domain of fs comb accuracy confirmation was provided by comparison of the apparent measured frequency of a HeNe I_2-stabilized laser, measured

[4] Here the averaging time is identical to the counter gate time. Because the dead time between counter readings was much larger than the inverse counter bandwidth juxtapositioning of say 1s gate time data to derive the Allan deviation for longer times would produce false results [43].

with a fs comb in JILA and with that measured by a traditional harmonic synthesis chain at NRC, Ottowa [44]. Expressing the difference between the two measurements of the 473 THz frequency of the Iodine-stabilized transfer laser, one found (200 ± 770 Hz). While the accuracy of this test (1.6×10^{-12}) has fewer digits, it is extremely comforting to find such an agreement between the two synthesis methods and the two national labs. (The domain below ≈ 1 kHz (2×10^{-12}) is hard to explore with the HeNe I_2 laser system, due to its broad line and rather large shifts with operating parameters).

9 The Fine Structure Constant α

Recently we have used the femtosecond technology to measure the transition frequency of the cesium D_1 line [45]. This line provides an important link for a new determination of the fine structure constant α. Because α scales all electromagnetic interactions, it can be determined by a variety of independent physical methods. Different values measured with comparable accuracy disagree with each other by up to 3.5 standard deviations and the derivation of the currently most accurate value of α from the electron $g-2$ experiment relies on extensive QED calculations [46]. The 1999 CODATA value [47] $\alpha^{-1} = 137.035\,999\,76(50)$ (3.7×10^{-9}) follows from the $g-2$ results. To resolve this unsatisfactory situation it is most desirable to determine a value for the fine structure constant that is comparable in accuracy with the value from the $g-2$ experiment but does not depend heavily on QED calculations. A promising way is to use the accurately known Rydberg constant R_∞ according to:

$$\alpha^2 = \frac{2R_\infty}{c}\frac{h}{m_e} = 2R_\infty \times \frac{2cf_{rec}}{f_{D_1}^2} \times \frac{m_p}{m_e} \times \frac{m_{Cs}}{m_p} \tag{15}$$

In addition to the Rydberg constant a number of different quantities, all based on intrinsically accurate frequency measurements, are needed. Experiments are under way in Stanford in S. Chu's group to measure the photon recoil shift $f_{rec} = f_{D1}^2 h/2m_{Cs}c^2$ of the cesium D_1 line [48]. Together with the proton-electron mass ratio m_p/m_e, that is known to 2×10^{-9} [49] and even more precise measurements of the cesium to proton mass ratio m_{Cs}/m_p in Penning traps, that have been reported recently [50], our measurement has already yielded a new value of α [45].

As shown in Fig. 7 we compared the frequency of the cesium D_1 line at 895 nm with the 4th harmonic of the methane stabilized He-Ne laser operating at 3.4 μm ($f = 88$ THz). The laser that creates the frequency comb, the fourth harmonic generation and the HeNe laser are identical with the systems shown in Fig. 4. However, the HeNe laser was stabilized to a methane transition in this experiment and was used as a frequency reference instead of the Cs fountain clock. The frequency of this laser has been calibrated at the Physikalisch Technische Bundesanstalt Braunschweig/Germany (PTB) and in our own laboratory [51] to within a few parts in 10^{13}.

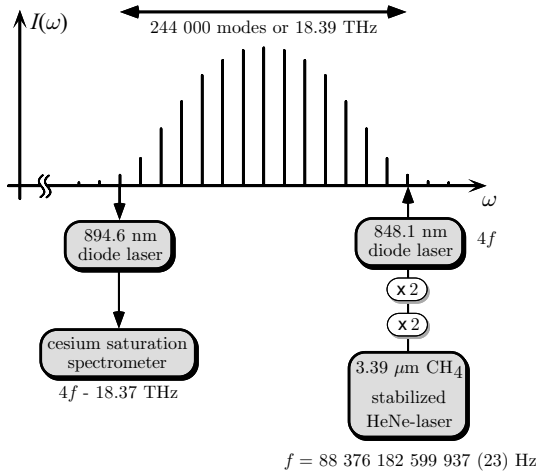

Fig. 7. Frequency chain used for the determination of the cesium D_1 line

10 Conclusion

To summarize we have presented here a new concept for measuring optical frequencies, based on a well-stabilized train of optical impulses. This new technique has been applied to the measurement of the hydrogen $1S-2S$ transition, to calibrate iodine stabilized HeNe lasers, and to the Cesium D_1 line which is a cornerstone for a new determination of α. This development culminates in the fully phase locked single-laser optical frequency synthesizer. It uses a single femtosecond laser and is nevertheless capable of phase coherently linking the rf domain with a whole octave of optical frequencies. It occupies only 1 square meter on our optical table with considerable potential for further miniaturization.

We believe that the development of accurate optical frequency synthesis marks only the beginning of an exciting new period of ultra-precise physics. The femtosecond frequency chain does also provide us with the long awaited compact optical clockwork that can serve in future optical clocks. Possible candidates for precise optical reference frequencies derived from narrow transitions in Ca, Hg^+ [52] and In^+ [53] are currently investigated using the femtosecond comb technology.

Acknowledgement

Finally the Garching group likes to thank their collaborators P. Lemonde, G. Santarelli, M. Abgrall, P. Laurent and A. Clairon from BNM-LPTF, Paris/France and J. Knight, W. Wadsworth, and P. Russell from the University of Bath, Bath/England. The JILA group thanks J. Ranka, R. Windeler, and A. Stenz of Lucent

Search Hits Help

BellLabs/USA, T.H. Yoon and L.S. Ma at JILA and in particular H.C. Kapteyn and M.M. Murnane for generous help with fs laser technology.

References

Note: In this discussion we have used the names of commercial products to facilitate technical communication with the reader. Such use in no way constitutes an endorsement of these products nor does it imply that other products would necessarily be less suitable.

1. J.N. Eckstein, A.I. Ferguson, and T.W. Hänsch: Phys. Rev. Lett. **40**, 847 (1978)
2. D.E. Spence, CP.N. Kean, and W. Sibbett: Opt. Lett. **16**, 42 (1991)
3. F. Krausz, M.F. Fermann, T. Brabec, P.F. Curley, M. Hofer, M.H. Ober, C. Spielmann, E. Wintner, and A.J. Schmidt: IEEE J. Quant. Electron. **28**, 2097 (1992)
4. M.T. Asaki, C.P. Huang, D. Garvey, J.P. Zhou, H.C. Kapteyn and M.M. Murnane: Opt. Lett. **18**, 977 (1993)
5. U. Morgner, F.X. Kärtner, S.H. Cho, Y. Chen, H.A. Haus, J.G. Fujimoto, E.P. Ippen, V. Scheuer, G. Angelow, and T. Tschudi: Opt. Lett. **24**, 411 (1999)
6. D.H. Sutter, L. Gallmann, M. Matuschek, F. Morier-Genoud, V. Scheuer, G. Angelow, T. Tschudi, G. Steinmeyer, and U. Keller: Appl. Phys. B **70**, 5 (2000)
7. J.C. Knight, T.A. Birks, P.St.J. Russell, and D.M. Atkin: Opt. Lett. **21**, 1547 (1996)
8. M.J. Gander, R. McBride, J.D.C. Jones, D. Mogilevtsev, T.A. Birks, J.C. Knight, and P.St.J. Russell: Electron. Lett. **35**, 63 (1999)
9. J.K. Ranka, R.S. Windeler, and A.J. Stentz: Opt. Lett. **25**, 25 (2000)
10. W.J. Wadsworth, J.C. Knight, A. Ortigosa-Blanch, J. Arriaga, E. Silvestre, and P.St.J. Russell: Electron. Lett. **36**, 53 (2000)
11. J.K. Ranka, R.S. Windeler, and A.J. Stentz: 'Efficient Visible Continuum Generation in Air-Silica Microstructure Optical Fibers with Anomalous Dispersion at 800 nm'. In: *Conference on Lasers and Electro-Optics CLEO*, postdeadline paper CD-8, Washington D.C. (1999)
12. W.J. Wadsworth, J.C. Knight, A. Ortigosa-Blanch, J. Arriaga, E. Silvestre, B.J. Mangan and P.St.J. Russell: 'Soliton Effects and Supercontinuum Generation in Photonic Crystal Fibres at 850 nm'. In: *Annual Meeting of IEEE Lasers and Optics Society, LEOS*, postdeadline paper PD1.5,
13. R. Holzwarth *et al.*: to be published.
14. S.A. Diddams, D.J. Jones, S.T. Cundiff, J.L. Hall, J.K. Ranka, R.S. Windeler, A.J. Stentz: 'A Direct rf to Optical Frequency Measurement with a Femtosecond Laser Comb spanning 300 THz'. In: *Quantum Electronics and Laser Science Conference QELS, OSA Technical Digest*, pp. 109-110.
15. R. Holzwarth, J. Reichert, Th. Udem, T.W. Hänsch, J.C. Knight, W.J. Wadsworth, P.St.J. Russell: 'Broadening of Femtsecond Frequency Combs and Compact Optical to Radio Frequency Conversion'. In: *Conference on Lasers and Electro-Optics CLEO, OSA Technical Digest*, p. 197.
16. J. Reichert, M. Niering, R. Holzwarth, M. Weitz, Th. Udem, and T.W. Hänsch: Phys. Rev. Lett. **84**, 3232 (2000)
17. S.A. Diddams, D.J. Jones, J. Ye, S.T. Cundiff, J.L. Hall, J.K. Ranka, R.S. Windeler, R. Holzwarth, Th. Udem, and T.W. Hänsch: Phys. Rev. Lett. **84**, 5102 (2000)

Search Hits Help

18. D.J. Jones, S.A. Diddams, J.K. Ranka, A. Stentz, R.S. Windeler, J.L. Hall, and S.T. Cundiff: Science **288**, 635 (2000)
19. R. Holzwarth, Th. Udem, T.W. Hänsch, J.C. Knight, W.J. Wadsworth, and P.St.J. Russell: Phys. Rev. Lett. **85**, 2264 (2000)
20. V.P. Chebotayev, and V.A. Ulybin: Appl. Phys. B **50**, 1 (1990)
21. J. Reichert, R. Holzwarth, Th. Udem, and T.W. Hänsch: Opt. Commun. **172**, 59 (1999)
22. R. Szipöcs, and R. Kohazi-Kis: Appl. Phys. **B 65**, 115 (1997)
23. J.N. Eckstein, thesis Stanford University, USA 1978.
24. D.J. Wineland, J.C. Bergquist, W.M. Itano, F. Diedrich, and C.S Weimer: 'Frequency Standards in the Optical Spectrum'. In: *The Hydrogen Atom* ed. by T.W. Hänsch (Springer, Berlin, Heidelberg 1989) pp. 123-133
25. L. Xu, Ch. Spielmann, A. Poppe, T. Brabec, F. Krausz, and T.W. Hänsch: Opt. Lett. **21**, 2008 (1996)
26. Th. Udem, J. Reichert, R. Holzwarth, and T.W. Hänsch: Opt. Lett. **24**, 881 (1999)
27. G.P. Agrawal: *Nonlinear Fiber Optics*, (Academic Press, New York 1989)
28. D. Milam: Applied Optics **37**, 546 (1998
29. K. Imai, M. Kourogi, and M. Ohtsu: IEEE Journal Quant. Electr. **34**, 54 (1998)
30. S.A. Diddams, D.J. Jones, L.S. Ma, S.T. Cundiff, and J.L. Hall: Opt. Lett. **25**, 186 (2000)
31. M. Niering, R. Holzwarth, J. Reichert, P. Pokasov, Th. Udem, M. Weitz, T.W. Hänsch, P. Lemonde, G. Santarelli, M. Abgrall, P. Laurent, C. Salomon, and A. Clairon: Phys. Rev. Lett. **84**, 5496 (2000)
32. P. Lemonde, P. Laurent, G. Santarelli, M. Abgrall, Y. Sortais, S. Bize, C. Nicolas, S. Zhang, A. Clairon, N. Dimarcq, P. Petit, A. Mann, A. Luiten, S. Chang, and C. Salomon: 'Cold Atom Clocks on Earth and in Space'. In: *Frequency Measurement and Control* ed. by A.N. Luiten (Springer, Berlin, Heidelberg 2000)
33. J. Ye, J.L. Hall, and S.A. Diddams: Opt. Lett. **25**, 1675 (2000)
34. D. McIntyre, T. W. Hänsch: *Digest of the Annual Meeting of the Optical Society of America*, paper ThG3, Washington D.C. (1988) and H.R. Telle, D. Meschede, and T.W. Hänsch: Opt. Lett. **15**, 532 (1990)
35. F. Biraben, T.W. Hänsch, M. Fischer, M. Niering, R. Holzwarth, J. Reichert, Th. Udem, M. Weitz, B.de Beauvoir, C. Schwob, L. Jozefowski, L. Hilico, F. Nez, L. Julien, O. Acef, and A. Clairon: *this book*, pp. 17–41
36. A. Huber, B. Gross, M. Weitz, and T.W. Hänsch: Phys. Rev. A **59**, 1844 (1999)
37. Th. Udem, A. Huber, B. Gross, J. Reichert, M. Prevedelli, M. Weitz, and T.W. Hänsch: Phys. Rev. Lett. **79**, 2646 (1997)
38. M. Bellini, T.W. Hänsch: Opt. Lett. **25**, 1049 (2000)
39. T. J. Quinn: Metrologia **36**, 211 (1999)
40. D. Touahri, O. Acef, A. Clairon, J.J. Zondy, R. Felder, L. Hilico, B. de Beauvoir, F. Biraben, and F. Nez: Opt. Comm. **133**, 471 (1997)
41. M. Kourogi, B. Widiyatomoko, Y. Takeuchi, and M. Ohtsu: IEEE J. Quantum Electron. **31**, 2120 (1995)
42. J.A. Barnes, A.R. Chi, L.S. Cutler, D.J. Healey, D.B. Leeson, T.E. McGunigal, J.A. Mullen Jr, W.L. Smith, R.L. Sydnor, R.F.C. Vessot, and G.M.R. Winkler: IEEE Trans. Instrum. Meas. **20**, 105 (1971)
43. P. Lesage: IEEE Trans. Instrum. Meas. **32**, 204 (1983)
44. J. Ye, T.H. Yoon, J.L. Hall, A.A. Madej, J.E. Bernard, K.J. Siemsen, L. Marmet, J.M. Chartier, and A. Chartier: Phys. Rev. Lett. **85**, 3739 (2000)
45. Th. Udem, J. Reichert, R. Holzwarth, and T.W. Hänsch: Phys. Rev. Lett. **82**, 3568 (1999)

46. T. Kinoshita: Rep. Prog. Phys. **59**, 1459 (1996), and references therein.
47. P.J. Mohr, and B.N. Taylor: Rev. Mod. Phys. **72**, 351 (2000)
48. A. Peters, K.Y. Chung, B. Young, J. Hensley, and S. Chu: Phil. Trans. R. Soc. Lond. A **355**, 2223 (1997)
49. D.L. Farnham, R.S. Van Dyck Jr, and P.B. Schwinberg: Phys. Rev. Lett. **75**, 3598 (1995)
50. M.P. Bradley, J.V. Porto, S. Rainville, J.K. Thompson, and D.E. Pritchard: Phys. Rev. Lett. **83**, 4510 (1999)
51. P. Pokasov *et al.*: to be published.
52. Th. Udem, S. Diddams, K. Vogel, C. Oates, A. Curtis, D. Lee, W. Itano, D. Wineland, J. Bergquist and L. Hollberg: to be published.
53. T. Becker, M. Eichenseer, A.Yu. Nevsky, E. Peik, C. Schwedes, M.N. Skvortsov, J. von Zanthier, and H. Walther: *this edition*, pp. 545–553